POLITECNICO DI TORINO
Repository ISTITUZIONALE

Spectral shaping of spreading sequences as a mean to address the trade-off between narrowband and multi-access interferences in UWB systems

(Article begins on next page)

Paper

Spectral shaping of spreading sequences as a mean to address the trade-off between narrowband and multi-access interferences in UWB systems

Mauro Mangia[1a]*, Fabio Pareschi*[2b]*, Riccardo Rovatti*[1c]*, and Gianluca Setti*[2d]

> [1] *ARCES, University of Bologna*
>   *via Toffano 2/2, Bologna, Italy*

> [2] *ENDIF, University of Ferrara*
>   *via Saragat 1, Ferrara, Italy*

> [a] *mmangia@arces.unibo.it*
> [b] *fabio.pareschi@unife.it*
> [c] *riccardo.rovatti@unibo.it*
> [d] *gianluca.setti@unife.it*

Abstract: This paper presents a way to cope with the need of simultaneously rejecting narrowband interference and multi-access interference in a UWB system based on direct-sequence CDMA. With this aim in mind, we rely on a closed-form expression of the system bit error probability in presence of both effects. By means of such a formula, we evaluate the effect of spectrum shaping techniques applied to the spreading sequences. The availability of a certain number of degrees of freedom in deciding the spectral profile allows us to cope with different configurations depending on the relative interfering power but also on the relative position of the signal center frequency and the narrowband interferer.

Key Words: UWB, DS-CDMA, narrowband interference, spectral shaping, linear probability feedback process, chaos

1. Introduction

Ultra Wide Band (UWB) systems play a key role in the efforts devoted to the design of the next generation communication infrastructure since they may help in addressing the basic need of a connectivity that should be, in principle, independent on the environment and as little supervised as possible.

UWB systems employ signals that feature a very low power density spectrum in order to appear almost equivalent to channel natural disturbances. To meet such a low power density request, and

at the same time, to deliver enough energy to the receivers, UWB systems fill large portion of the spectrum, thus almost surely overlapping with other systems or services, being them either wideband or narrowband.

Coexistence in such shared, unsupervised environment depends on the ability of narrowband systems to tolerate an increased noise floor (possibly increasing their power budget) and on the capability of the wideband systems to reject narrowband interference (possibly adapting their transmission scheme to time-varying scenarios).

The point addressed in this paper is the second one, i.e., when the UWB signals are involved in a Direct-Sequence spread spectrum transmission with Multiple Access based on Code Division (DS-CDMA). Such a classical technique [1] may allow arbitrary spreading and is suitable for extremely simple implementations of both transmitter and receiver.

In our scenario, the narrowband interferer may be either an intentionally emitted jammer or the abstract subsumption of the effects of a traditional non-UWB service and, for the sake of simplicity, it is modeled as a single sinusoidal tone.

Among all the possible figures of merit that quantify the performance of communication (e.g., multipath robustness, system capacity in terms of users number [2]) we concentrate on the joint effect of Multiple Access Interference (MAI) and NarrowBand Interference (NBI) on a simple Matched Filter (MF) receiver.

Our starting point is the result reported in [3] that expresses the performance of a conventional DS-CDMA system with no multi-access when it is disturbed by a jamming tone. Such a result is extended to take into account the presence of a noise-like disturbance due to other asynchronous users whose spreading codes cannot be perfectly orthogonal to the useful receiver one for all the possible time shifts. This disturbance has been also extensively investigated in classical DS-CDMA and UWB systems relying on possible spreading codes optimizations based on chaotic systems (piece-wise affine markov maps; see [4,5] for a survey on chaos-based sequences generation for various applications), both in Additive White Gaussian Noise (AWGN) channels [6–17] and in presence of multipath [18–21]. The influence of real pulse shapes has been also taken into account [22–25], while the ultimate
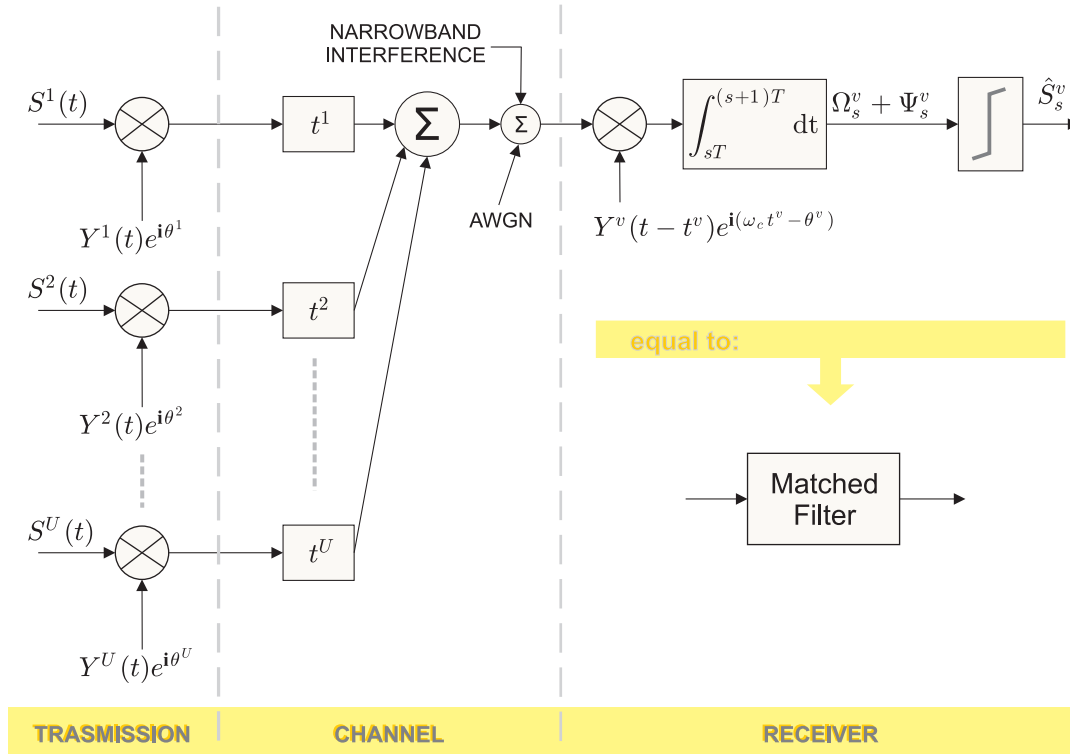

Fig. 1. Block diagram of the baseband equivalent scheme of a UWB asynchronous DS-CDMA system.

limit of these systems in terms of Shannon capacity is studied in [26, 27].

Here, we extend the results presented in [28] and show how the rejection of both narrowband interference and multi-access disturbance can be achieved by the proper spectrum shaping of the spreading codes towards different optimal profiles. Furthermore, we here also address the trade-off between the two optimal designs for different scenarios as far as the power of the narrowband jammer and the number of competing users are concerned. Different optimal solutions will be found depending on the relative interfering power but also on the relative positioning of the signal center frequency and the jammed frequency.

The paper is organized as follows. In Section 2, we describe the model of an UWB DS-CDMA system and express its performance in terms of bit error probability on a single link when MAI, NBI and thermal noise are the main cause of non-ideality. In Section 3 we present the idea to reduce the impact of NBI without increasing the impact of MAI, and we show in Section 4 how we can generate spreading sequences capable to do this. Finally, in Section 5, we report the results of Montecarlo simulations clarifying the scenarios in which our method offers significant improvement.

2. System model

The starting point of our analysis is the model of a standard asynchronous DS-CDMA system [1, 8] including transmission module, channel and receiver. Figure 1 shows a simplified baseband equivalent scheme including the effects of thermal channel noise (modeled as AWGN) and NBI, in addition to MAI. To evaluate system performance, let us assume the presence of a common carrier with frequency $f_c = \omega_c/(2\pi)$, let U be the total number of users, and express the generic u-th information signal as

$$S^u(t) = V \sum_{s=-\infty}^{\infty} S_s^u g_T(t - sT) \tag{1}$$

where T is the bit duration, $S_s^u \in \{-1; +1\}$ is the s-th information symbol for the u-th user, g_T is a rectangular pulse which is 1 within $[0; T]$ and zero otherwise, and where the peak amplitude V is assumed equal for all users. The signal $S^u(t)$ is then multiplied by the spreading signal

$$Y^u(t) = \sum_{s=-\infty}^{\infty} y_s^u g_{T/N}\left(t - s\frac{T}{N}\right) \tag{2}$$

where N is the spreading factor, y_s^u are the antipodal spreading symbols of the u-th user and $g_{\frac{T}{N}}$ is a rectangular pulse which is 1 within $[0; \frac{T}{N}]$ and 0 outside, and where, following the approach in [1, 8], we will assume that the corresponding Spreading Sequence (SS) $\underline{y}^u = \{y_s^u\}$ is periodic, with period equal to N.

The resulting signal is then transmitted along the (baseband equivalent) channel together with the spread-spectrum signals from the other users. Each transmitter adopts a different spreading code, assigned at the connection start-up. The receiver is a simple MF which is made of a multiplier combining the incoming signal with a synchronized replica of the spreading sequence of the v-th user and of an integrate-and-dump stage in charge of extracting the information symbol by correlation.

For each user we consider a different delay t^u and a different phase θ^u. These quantities are assumed as uniformly distributed random variables to model transmission from mobile terminals to a fixed base-station. If we take the v-th receiver as a reference, we can define the relative delays $\Delta t^{uv} = t^u - t^v$ and the relative phase $\Delta \theta^{uv} = \theta^u - \theta^u$.

We do this to arrive at the expression of the contribution of the u-th user to the signal produced by the v-th MF, given by

$$\Upsilon_s^{uv} = \frac{1}{2T} \int_{sT}^{(s+1)T} S^u(t - \Delta t^{uv})Y^u(t - \Delta t^{uv})Y^v(t)e^{\mathbf{i}\Delta\theta^{uv}}dt \tag{3}$$

where $\mathbf{i}$ is the imaginary unit.

In the following we will assume that the system performance is mainly limited by MAI, thermal noise and NBI, namely we will suppose that spreading-despreading sequence synchronization has

been achieved, and that multipath effects are negligible. Despite these simplifying assumptions, performance computation is quite difficult in this case, and, in order to obtain a suitable model, we rely on two previous results corresponding to "corner" cases where either NBI and thermal noise or MAI are present alone, as presented in Subsection 2.1 and Subsection 2.2, respectively.

2.1 Multiple access interference

We want to evaluate in terms of bit error probability the impact of MAI, and to this purpose, we define the *partial cross-correlation* function between two generic spreading sequences $\underline{y}^u = \{y_k^u\}$ and $\underline{y}^v = \{y_k^v\}$ as

$$\Gamma_{N,\tau}(\underline{y}^u, \underline{y}^v) = \begin{cases} \sum_{k=0}^{N-\tau-1} y_k^u y_{k+\tau}^v & \text{if } \tau = 0, 1, \ldots, N-1 \\ \Gamma_{N,-\tau}(\underline{y}^v, \underline{y}^u) & \text{if } \tau = -N+1, \ldots, -2, -1 \\ 0 & \text{if } |\tau| \geq N \end{cases}$$

Exploiting the previous expression, we can use (3) to write the useful signal component as

$$\Omega_s^v = \Upsilon_s^{vv} = \frac{V S_s^v}{2T} \int_{sT}^{(s+1)T} [Y^v(t)]^2 dt = \frac{V S_s^v}{2N} \Gamma_{N,0}(\underline{y}^v, \underline{y}^v) = \frac{V S_s^v}{2}$$

and the interfering signal component (which depends on MAI)

$$\Psi_s^v = \sum_{\substack{u \neq v \\ u=1}}^{U} \Upsilon_s^{uv} = \sum_{\substack{u \neq v \\ u=1}}^{U} \frac{1}{2T} \int_{sT}^{(s+1)T} S^u(t - \Delta t^{uv}) Y^u(t - \Delta t^{uv}) Y^v(t) e^{\mathbf{i}\Delta\theta^{uv}} dt \quad (4)$$

We can assume that the information symbols are independent identically distributed random variable. This brings us to the following expression [8, 10]

$$\Psi_s^v = \frac{1}{2N} \sum_{\substack{u \neq v \\ u=1}}^{U} V e^{\mathbf{i}\Delta\theta^{uv}} \Bigg\{$$

$$S_{s-1}^u \left[\left(\frac{\Delta t^{uv}}{T} - \left\lfloor \frac{\Delta t^{uv}}{T} \right\rfloor \right) \Gamma_{N, \lfloor \frac{\Delta t^{uv}}{T} \rfloor - N+1}(\underline{y}^u, \underline{y}^v) + \left(1 - \frac{\Delta t^{uv}}{T} + \left\lfloor \frac{\Delta t^{uv}}{T} \right\rfloor \right) \Gamma_{N, \lfloor \frac{\Delta t^{uv}}{T} \rfloor - N}(\underline{y}^u, \underline{y}^v) \right] +$$

$$+ S_s^u \left[\left(\frac{\Delta t^{uv}}{T} - \left\lfloor \frac{\Delta t^{uv}}{T} \right\rfloor \right) \Gamma_{N, \lfloor \frac{\Delta t^{uv}}{T} \rfloor + 1}(\underline{y}^u, \underline{y}^v) + \left(1 - \frac{\Delta t^{uv}}{T} + \left\lfloor \frac{\Delta t^{uv}}{T} \right\rfloor \right) \Gamma_{N, \lfloor \frac{\Delta t^{uv}}{T} \rfloor}(\underline{y}^u, \underline{y}^v) \right] \Bigg\}$$

where, $\Delta\theta^{uv} \in [-\pi; \pi]$ and the normalized delay $\frac{\Delta t^{uv}}{T}$ has been split into a integer part $\left\lfloor \frac{\Delta t^{uv}}{T} \right\rfloor$ and a fractional part $\frac{\Delta t^{uv}}{T} - \left\lfloor \frac{\Delta t^{uv}}{T} \right\rfloor$. Since the interference term is a sum of many zero-mean independent random variables, we can model it as zero-mean Gaussian random variable, whose variance is equal to [8, 10]

$$(\sigma^v)^2 = \mathbf{E}[(\Psi_s^v)^2] = \sum_{\substack{u \neq v \\ u=1}}^{U} \frac{(V)^2}{24N^3} \sum_{j=-N+1}^{N-1} \left(2\Gamma_{N,j}^2(\underline{y}^u, \underline{y}^v) + \Gamma_{N,j}(\underline{y}^u, \underline{y}^v) \Gamma_{N,j+1}(\underline{y}^u, \underline{y}^v) \right)$$

where the expectation $\mathbf{E}[\cdot]$ is taken over the phase $\Delta\theta^{uv}$, the delay Δt^{uv} (that is assumed uniformly distributed in $[-T; T]$) and the information symbols S_s^u (that are assumed independent and equally distributed, so that $S_s^u = -1$ and $S_s^u = +1$ have the same probability).

MAI for the v-th link is proportional to $(\sigma^v)^2$, so that we can evaluate the performance in terms of bit-error probability for the s-th transmitted symbol as $P_{err}^v = \frac{1}{2}\text{erfc}\sqrt{(\Omega_s^v)^2/[2(\sigma^v)^2]} = \frac{1}{2}\text{erfc}\sqrt{V^2/[8(\sigma^v)^2]}$. The overall system performance can be obtained by averaging over all possible useful users v by defining

$$\text{BEP}_{\text{MAI}} = \mathbf{E}_{\underline{y}^v}[P_{err}^v] = \frac{1}{2}\mathbf{E}_{\underline{y}^v}\left[\text{erfc}\sqrt{\frac{V^2}{8(\sigma^v)^2}}\right]$$

where $\mathbf{E}_{\underline{y}^v}[\cdot]$ is the expectation over the set of sequences. Analytical handing is difficult due the presence of the erfc function. A common workaround to this is to use the Standard Gaussian Approximation (SGA) which considers the spreading codes values as random variables (see [1] and [29] for an in-depth analysis of this approximation) to simplify the above expression in

$$\text{BEP}_{\text{MAI}} \approx \frac{1}{2}\text{erfc}\sqrt{\frac{V^2}{8\,\mathbf{E}_{\underline{y}^v}[(\sigma^v)^2]}}$$

Working on the inner expectation we get [8, 10]

$$\mathbf{E}_{\underline{y}^v}[(\sigma^v)^2] = \frac{U-1}{3N^3}\sum_{j=-N+1}^{N-1}\mathbf{E}_{\underline{y}^u,\underline{y}^v}^{u\neq v}\left[2\Gamma_{N,j}^2(\underline{y}^u,\underline{y}^v) + \Gamma_{N,j}(\underline{y}^u,\underline{y}^v)\Gamma_{N,j+1}(\underline{y}^u,\underline{y}^v)\right]$$

so that, by defining R,

$$\text{R} = \frac{1}{3N^3}\sum_{j=-N+1}^{N-1}\mathbf{E}_{\underline{y}^u,\underline{y}^v}^{u\neq v}\left[2\Gamma_{N,j}^2(\underline{y}^u,\underline{y}^v) + \Gamma_{N,j}(\underline{y}^u,\underline{y}^v)\Gamma_{N,j+1}(\underline{y}^u,\underline{y}^v)\right]$$

we come to the final expression

$$\text{BEP}_{\text{MAI}} \approx \frac{1}{2}\text{erfc}\sqrt{\frac{V^2}{(U-1)\text{R}}} \tag{5}$$

which allows us to interpret Ras an *expected interference-to-signal ratio per interfering user*, i.e., an expected degradation in system performance when a new user is added.

The expression of R can be further simplified taking into account that we are using antipodal symbol for the spreading sequences. More specifically, assuming second-order stationary sequences, i.e. such that $\mathbf{E}_{\underline{y}^v}[y_m^v y_n^v] = \mathbf{E}_{\underline{y}^v}[y_0^v y_{|m-n|}^v]$, we may use the auto-correlation function $A_k = \mathbf{E}_{\underline{y}^v}[y_0^v y_k^v]$ to write, with few algebraic manipulation [10], an alternative expression of R depending only on A_k and N, namely

$$\text{R} = \frac{2}{3N} + \frac{4}{3N^3}\sum_{k=1}^{N-1}\left[(N-k)^2 A_k^2 + \frac{(N-k+1)(N-k)}{2}A_k A_{k-1}\right] \tag{6}$$

In [12] R is minimized and minimally interfering sequences are approximated by those with $A_k \approx r^k$ where $r = -2 + \sqrt{3}$, which can easily be generated by suitable piece-wise affine Markov maps [4]. In other terms, chaos-based spreading sequences can be generated, whose adoption allows to optimize performance in asynchronous (UWB) DS-CDMA systems when MAI is the main cause of non-ideality and we will use this case as a benchmark in our present study.

2.2 Narrowband interference and thermal noise

For the present study, symbol recovery is hindered not only by MAI, but also by the presence of thermal noise and, most important, by an NBI, which models either an intentional jamming or a conventional non spread-spectrum transmissions, or both.

For this scenario, we consider the impact of NBI and thermal noise on v-th user, where the former is expressed as a single sinusoidal jamming signal $\sqrt{2I}\cos(2\pi f_0 t + \phi_0)$, of (normalized baseband equivalent) frequency f_0, initial phase ϕ_0 and transmitted power I. Hence, relying on [3] one can compute performance in terms of bit error probability as

$$\text{BEP}_{\text{I}} = \frac{1}{2} - \frac{1}{\pi}\int_0^\infty J_0\left(\omega\sqrt{\frac{I}{C}\frac{|H^v(f_0)|^2}{2T}}\right)\frac{\sin\omega}{\omega}e^{\left(-\frac{\omega^2}{4}\frac{N_0}{E_b}\right)}d\omega \tag{7}$$

where $J_0(\omega)$ is the 0-th order Bessel function of the first kind, E_b is the transmitted energy per information symbol, $C = E_b/T$ denotes the corresponding useful received power, and thermal noise is modeled as a two-sided power spectral density equal to $N_0/2$. Furthermore, $H^v(f)$ is the transfer function of the MF for v-th link and represents the Fourier transform of $(b(t;-1) - b(t;+1))$, where $b(t;\pm1)$ is equal to a unit-energy waveform used to transmit the information symbol -1 or $+1$. To find its expression, let us express the unit-energy waveform of the v-th user as

$$b^v(t) = \sqrt{\frac{2}{NE_g}} \sum_{j=0}^{N-1} y_j^v g_{\frac{T}{N}}\left(t - j\frac{T}{N}\right)$$

so that, exploiting the fact that the a chip waveform energy is $E_g = T/N$, the desired transfer function can be written as

$$|H^v(f_0)| = N\sqrt{2T}\left|\text{sinc}\left(f_0\frac{T}{N}\right)\right|\left|\sum_{s=0}^{N-1} y_s^v e^{-2\pi\mathbf{i}\, f_0 k \frac{T}{N}}\right|$$

2.3 All causes of error

The aim of this section is to obtain a final expression of the system performance in terms of bit error probability, similar to (5) and (7), and which includes all considered causes of error at the same time. To do this, we may first note that, within the limit of validity of SGA, MAI is a Gaussian random variable whose effect on system performance is similar to thermal noise. Consequently, we may equivalently model the effect of both MAI and thermal noise exploiting (7) if we suitably increase the noise power spectral density from N_0 to $\tilde{N}_0$. The same effect of MAI at the output of the MF is obtained if, taking into account that $\int_{-1/T}^{1/T} |H^v(f)|^2 df = C$ for each SS, we impose

$$\frac{\tilde{N}_0}{2} = \frac{N_0}{2} + \frac{(U-1)\text{R}}{C}$$

With this, we finally arrive to express the system performance in presence of NBI, MAI and thermal noise as

$$\text{BEP}^v = \frac{1}{2} - \frac{1}{\pi}\int_0^\infty J_0\left(\omega\sqrt{\frac{I}{\text{C}}\frac{|H^v(f_0)|^2}{2T}}\right)\text{sinc}(\omega)\cdot\exp\left(-\frac{\omega^2}{4}\cdot\frac{N_0 + 2(U-1)\text{R}/C}{E_b}\right)d\omega \qquad (8)$$

As a final remark, we need to note that (8) depends on the particular choice of the spreading sequence of the v-th useful user. Regrettably the analytic evaluation of $\mu(\text{BEP}^v) = \mathbf{E}_{y^v}[\text{BEP}^v]$ is prohibitive from an analytic point of view and we will therefore rely, in Section 5, on its numerical evaluation based on a Montecarlo approach.

3. NBI reduction

The main idea to reduce the effect of NBI in a DS-CDMA UWB communication relies on the dependence of BEP^v in (8) on the SS, whose statistical features need thus to be appropriately chosen to achieve such a goal.

The starting point of our procedure, that is described in [12, 17], is a chaos-based technique able to generate antipodal SSs with autocorrelation profile $A_k \approx (-2 + \sqrt{3})^k$, whose adoption leads to a minimum level of MAI and therefore of R. Figure 2 shows the normalized Power Spectral Density (PDS) of such sequences (solid line), which therefore gives an indication of the shape of the MF transfer function of the receiver. If the vertical thick line represents the NBI, it is therefore evident that a consistent part of its power is transferred at the output of the MF, i.e., at the input of the decision block, thus increasing the error probability. To cope with this, the most intuitive solution is to use SSs whose PSD features a stop-band in a (large-enough) neighborhood of the NBI frequency, as it is also shown in Fig. 2(dashed line).

Note that we have also assumed that the NBI frequency is fixed and known. This is not a critical hypothesis since the aim of this work is to minimize the possible interference of existing narrowband communication systems on a UWB system working in the same band.
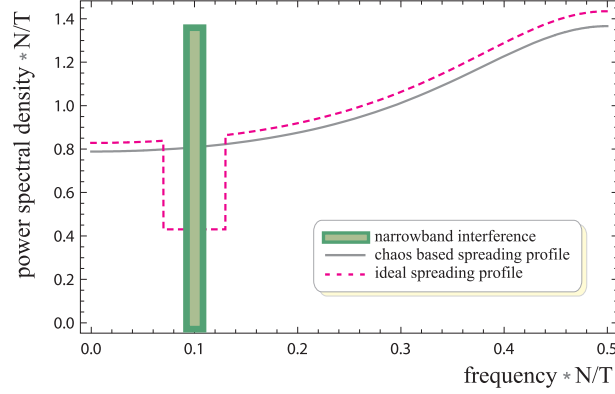
Fig. 2. Normalized PSD of the chaos-based spreading sequence minimizing (5) (solid line), jamming signal with $f_0 = 0.1N/T$ (thick solid line) and ideal PSD of spreading sequences capable of minimizing the effect of the NBI at the v-th useful user receiver (dashed line).

Two issues are worth mentioning. On the one hand, independently of the method used to generate spreading sequences, those satisfying the above PSD condition will certainly not be the same that minimize R. This will result in an increased MAI with respect to optimal chaos-based spreading [12] so that the possibility of achieving an improvement in performance will critically depend on the effectiveness in suppressing NBI and on its intensity. On the other hand, as shown in [4], the (binary) quantized output of a one-dimensional chaotic map can exhibit only a low-pass, high-pass or flat PSD, so that SSs with a PSD similar to the one represented by the dashed-line of Fig. 2 can be only obtained through a much more complex generator. The structure of one of such generator is described in the next Subsection.

4. Sequences generator

To obtain spreading sequences with assigned spectral profile we will rely on a Linear Probability Feedback Process (LPFP) recently introduced in [30, 31], whose scheme is shown in Fig. 3(a). It is based on a causal time-invariant linear filter with impulse response h_k such that $h_k = 0$ for $k \leq 0$ and transfer function

$$H_m(z) = \sum_{k=1}^{m} h_k z^{-k}$$

Though, in principle, there is no need for m to be a finite number, we will make this assumption here. The output of the filter $-H_m(z)$ produces the process $x_t = -\sum_{k=1}^{m} h_k y_{t-k}$. We will assume that $-1 \leq x_t \leq 1$, since, being the y_t antipodal symbols, this is equivalent to impose the constraint

$$\sum_{k=1}^{m} |h_k| \leq 1 \tag{9}$$

The process x_t is then fed into a comparator and matched with the process α_t that is made of independent random thresholds uniformly distributed in $[-1, 1]$. The comparator yields the antipodal values $y_t \in \{-1, 1\}$ that are fed back into the filter to allow a continuous generation of symbols. Assuming the uniform cumulative distribution function

$$F(\alpha) = \begin{cases} 0 & \text{if } \alpha < -1 \\ \frac{1+\alpha}{2} & \text{if } -1 \leq \alpha \leq 1 \\ 1 & \text{if } \alpha > 1 \end{cases}$$

for each random variables α_t in the scheme, we can write the probability of the current generated symbol y_t given the previous sequence with memory m as

$$\Pr\{y_t = +1 | y_{t-1}, y_{t-2}, \ldots, y_{t-m}\} = F\left(-\sum_{k=1}^{m} h_k y_{t-k}\right) = \frac{1}{2}\left[1 - \sum_{k=1}^{m} h_k y_{t-k}\right] \tag{10}$$
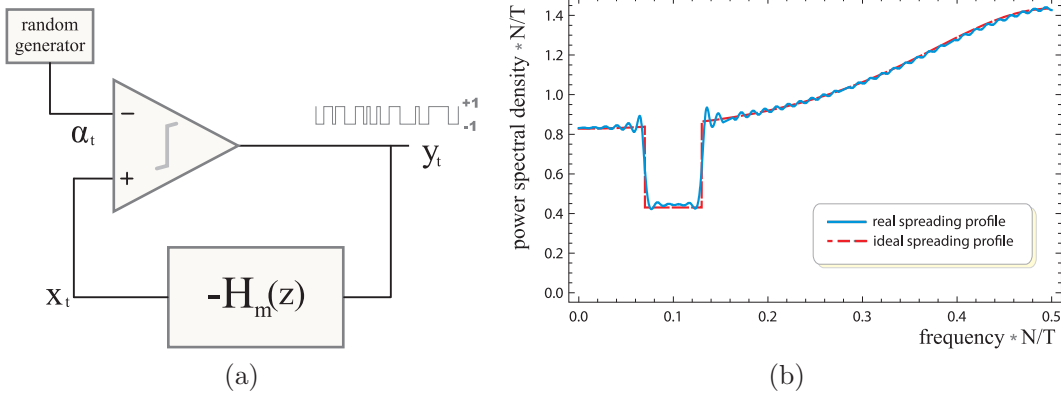
Fig. 3. (a) Structure of a memory-m antipodal linear probability feedback process generator, including a finite memory filter $-\mathrm{H}_m(z)$, a random generator and a comparator. (b) Normalized ideal PSD compared with the actual one obtained using the memory-m antipodal linear probability feedback process generator.

As discussed in details in [30], starting from (10) a thorough analysis leads to an expression of the normalized power spectral density of the generated antipodal symbols y_t, namely

$$\Lambda_y(f) = \frac{\left|1 + H_m(e^{2\pi \mathbf{i} f})\right|^{-2}}{\int_{-1/2}^{1/2} \left|1 + H_m(e^{2\pi \mathbf{i} f})\right|^{-2} df} \tag{11}$$

In principle one could use (11) to derive h_k once $\Lambda_y(f)$ has been set to a desired PSD profile similar to the one shown in Fig. 2. Regrettably, inverting (11) is a prohibitive task. To cope with this we note that if the process y_t is fed into a filter with transfer function $1 + H_m(f)$, the output is a white process with power spectral density equal to

$$P = \frac{1}{\int_{-1/2}^{1/2} \left|1 + H_m(e^{2\pi \mathbf{i} f})\right|^{-2} df}$$

so the whitening filter of y_t is $1 + H_m(z)$. From this we get that $-H_m(z)$ must be the optimum linear predictor of y_t that can be derived minimizing

$$\epsilon^2 = \mathbf{E}\left[\left(y_t + \sum_{k=1}^{m} h_k y_{t-k}\right)^2\right] = C_{0,0} + 2\sum_{k=1}^{m} C_{k-1,0} h_k + \sum_{k=1}^{m}\sum_{j=1}^{m} C_{k-1,j-1} h_k h_j$$

where $C_{k,j}$ is the correlation matrix of the process y_t, defined as

$$C_{k,j} = \mathbf{E}[y_{t-k} y_{t-j}] = \int_{-1/2}^{1/2} \Lambda_y(f) e^{2\pi \mathbf{i}(k-j)f} df = \int_{-1/2}^{1/2} \Lambda_y(f) \cos(2\pi(k-j)f) df$$

To solve this problem, we can use the classic approach based on Yule-Walker equations. Regrettably the solution, in general, do not satisfy (9). A numerical method such as a modified gradient descent was presented in [30] and more sophisticated heuristic techniques are used in [31].

As an example, exploiting the first technique with $m = 80$ we have been able to obtain spreading sequences whose normalized PSD is shown in Fig. 3(b) (continuous line). As it can be seen, the shape is almost superimposing with the target one (dashed line).

Note also that the presented method generates sequences with stationary statistical features, but this is not a limit in our case since we are supposing that the NBI frequency is fixed and know.

5. Numerical results

As discussed at the end of Section 2, Eq. (8) shows that the performance of the v-th user in terms of bit error probability BEP^v is actually a random variable that depends in a non-linear way on the
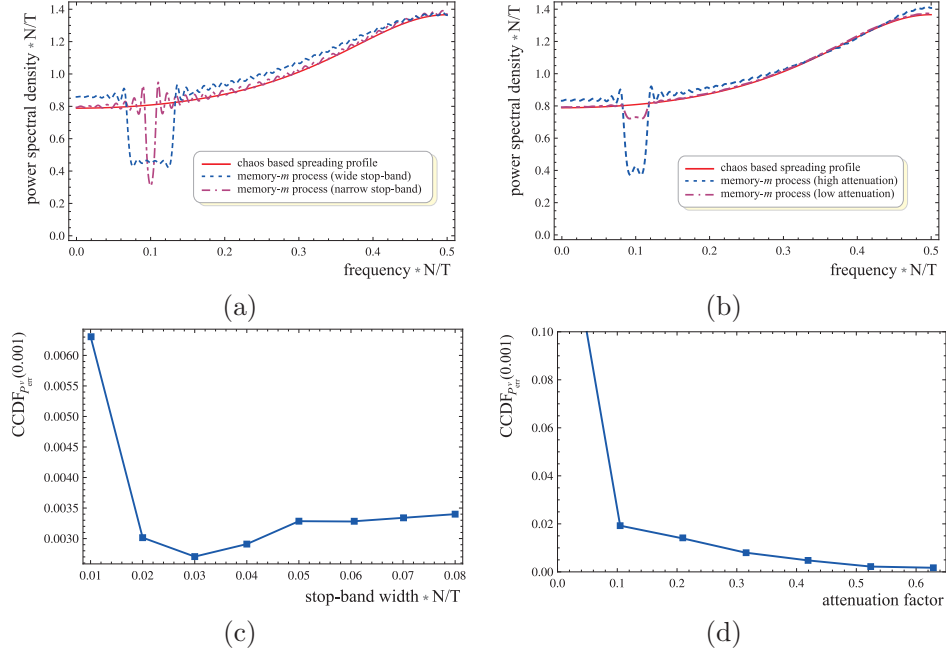
Fig. 4. Plot (a) and (b) show the PSD associated to chaos-based spreading sequences minimizing MAI (continous-line) and those generated by an LPFP with $m = 80$ targeting stop-bands with different widths and depths to reduce NBI (dotted and dash-dotted lines). Plot (c) and (d) show $\text{CCDF}_{P_{\text{err}}^v}(10^{-3})$ as a function of the stop-band width and the attenuation factor ρ (related to the stop-band depth), considering SIR= -12 dB, SNR= 20 dB, $f_0 = 0.1N/T$, $U = 12$.

spreading sequence $\underline{y}^v$. Consequently, to evaluate the effectiveness of the NBI reduction methodology proposed in this paper, we must rely on a statistical characterization of BEP^v by means of Montecarlo simulations.

To collect statistics for the generic v-th user and for a given system configuration, we first generate 2×10^5 spreading sequences using the LPFP discussed in Section 4 for a fixed spectral shape. Then we compute the corresponding instance of BEP^v exploiting (8), where R is evaluated through (6) using the autocorrelation function corresponding to the chosen spectral profile. As a realistic setting, following [3], we refer to an asynchronous DS-CDMA system with $T = 100$ ns, $N = 128$ (so that the spreading bandwidth is $N/T = 1.28$ GHz), and where the thermal noise power is relatively low (SNR= $E_b/N_0 = 20$ dB).

As a first step, we consider the relationship between the bit error probability and the width and depth of the introduced stop-band in the spectral profile. Figure 4(a) shows the spectral profile of the generated sequences with maximum (dashed line) and minimum (dash-dotted line) width, while Fig. 4(b) shows similar figures used to investigate the role of stop band depth. In both figures the solid line is the considered benchmark, namely the PSD profile of chaos-based spreading sequences minimizing MAI only.

We refer to a system where $U = 12$ users are present, with a signal-to-interference-ratio SIR= $C/I = -12$ dB and where the NBI is centered in a neighborhood of $f_0 = 0.1N/T$. In this setting, the NBI plays an important role and its reduction is therefore expected to show appreciable effects, making it easier to find an optimum value of the stop-band width and of the stop-band depth.

Focusing on the stop-band depth, let us define the attenuation factor ρ for a fixed NBI frequency, namely

$$\rho = \frac{\text{PSD}^{\text{chaos}-\text{based}}(f_0) - \text{PSD}^{\text{memory}-m}(f_0)}{\text{PSD}^{\text{chaos}-\text{based}}(f_0)}$$

The figure of merit we chose is the Complementary Cumulative Distribution Function (CCDF) of BEP^v, defined as $\text{CCDF}_{P_{\text{err}}^v}(\delta) = \Pr\{\text{BEP}^v > \delta\}$, which we will computed for the typical case of $\delta = 10^{-3}$. Let us refer to the results shown in Figs. 4(c) and (d). Plot (c) represents $\text{CCDF}_{P_{\text{err}}^v}(10^{-3})$
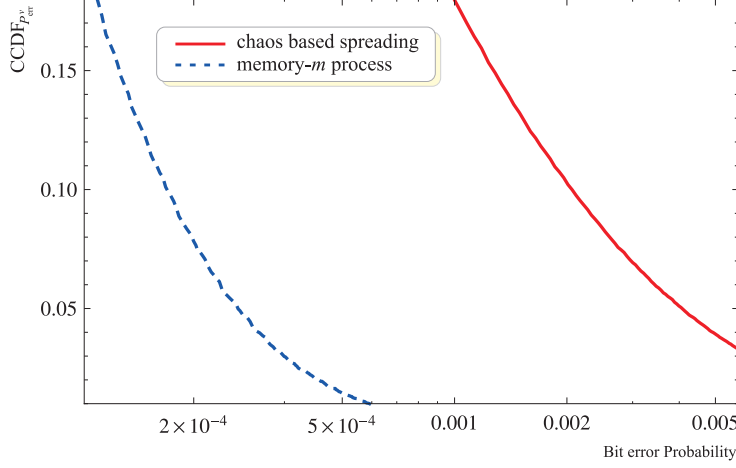
Fig. 5. The $\text{CCDF}_{P_{\text{err}}^v}$ as a function of BEP, with: stop-band width $= 0.03N/T$, attenuation factor $\rho = 0.62$, SIR$= -12$ dB, SNR$= 20$ dB, $f_0 = 0.1N/T$, $U = 12$.

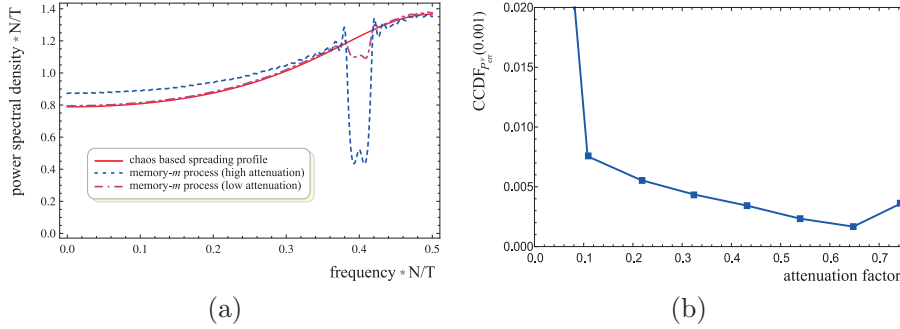(a)   (b)

Fig. 6. (a) PSD associated to chaos-based spreading sequences minimizing MAI (continous-line), and generated by LPFP with $m = 80$ targeting stop-band with different depth to reduce NBI (dashed and dot-dashed lines. (b) $\text{CCDF}_{P_{\text{err}}^v}(10^{-3})$ as a function of the attenuation factor, considering: SIR$= -3$ dB, SNR$= 20$ dB, $f_0 = 0.4N/T$, $U = 20$.

as a function of the normalized stop-band width, clearly showing a minimum for the optimal width value equal to $0.03N/T$ (corresponding to 39.322 MHz). It is worth noting that we investigate only a limited range for the stop-band width, as shown in Fig. 4(a). In fact, on the one end, for larger stop-bands the resulting SS profiles would be too much close to uniform and therefore too different with respect to the one minimizing the effect of MAI. On the other end, a narrower stop-bands would bring negligible advantage in NBI reduction.

Figure 4(d) shows that $\text{CCDF}_{P_{\text{err}}^v}(10^{-3})$ is always decreasing with the attenuation factor ρ. Hence the optimal value would apparently correspond to $\rho = \rho_{\max} = 1$, for which $\text{PSD}^{\text{memory}-m}(f_0) = 0$. Yet, such a lower value of $\text{PSD}^{\text{memory}-m}(f_0)$ cannot be achieved with LPFPs, since they are characterized by an almost-everywhere non-null PSD [30]. Consequently, for practical purposes, we will use an upper bound for ρ equal to the maximum value which guarantees correct generation of the SS via an LPFP ($\rho = 0.62$ in this setting).

Figure 5 represents $\text{CCDF}_{P_{\text{err}}^v}(\text{BEP})$ computed for the optimal values of the stop-band width and of the attenuator factor ρ mentioned above. It can be clearly seen that memory-m sequences always offer an advantage with respect to chaos-based ones, with an improvement in reducing $\text{CCDF}_{P_{\text{err}}^v}$ of at least 30%.

As a further step, we analyze the influence on system performance of the number of users U (on which MAI directly depends, see (5)), of SIR (whose increment reduces NBI) and of f_0. The latter parameter plays a particularly important role. In fact, since the PSD of optimal chaos-based spreading is high-pass (see the continuous-line in Figs. 4(a) and (b)), one may intuitively accept that when $f_0 < N/2T$, the presence of a stop-band introduces a negligible perturbation of the profile
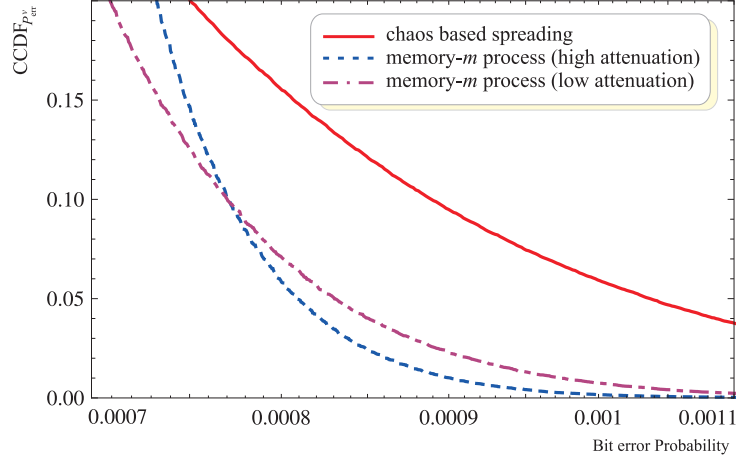
Fig. 7. The CCDF$_{P^v_{\mathrm{err}}}$ as a function of BEP, with: stop-band width = $0.03N/T$, SIR= -3 dB, SNR= 20 dB, $f_0 = 0.1N/T$, $U = 20$.
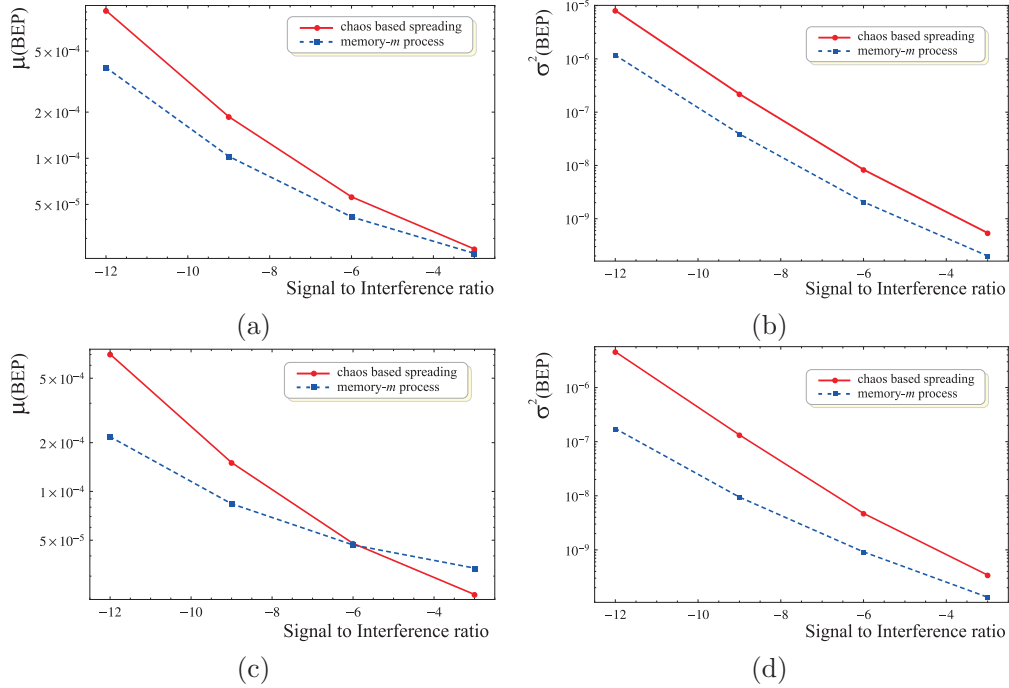

Fig. 8. Plot (a) and (b) show mean and variance of BEP with: stop-band width = $0.03N/T$, $\rho = 0.62$, SNR= 20 dB, $f_0 = 0.1N/T$, $U = 12$. Plot (c) and (d) show mean and variance of BEP with: stop-band width = $0.03N/T$, $\rho = 0.65$, SNR= 20 dB, $f_0 = 0.4N/T$, $U = 20$.

with respect to the one minimizing MAI. Consequently, as one may expect, results of all performed numerical simulations confirm that the optimal width for the stop band is always close to the one corresponding to the minimum value in Fig. 4(c). On the contrary, the influence of ρ is different, as reported in Figs. 6(a), (b) where, with respect to the previous case, $U = 20$, SIR= -3 dB and $f_0 = 0.4N/T$. As it can be noticed, the optimal value of the attenuation factor is $\rho = 0.65$, i.e., it is no more coincident with the maximum value compatible with the LPFP generation method.

The associated results in terms of CCDF$_{P^v_{\mathrm{err}}}$ are shown in Fig. 7, where the dashed and the dot-dashed lines correspond respectively to $\rho = 0.65$ (optimum value for BEP$^v = 10^{-3}$) and $\rho = 0.12$. It is interesting noticing that the proposed method always improves performance with respect to chaos-based spreading (continuous-line), but the actual improvement depends on the choice of ρ.

Given the above results, one may therefore conclude that, in any given scenario scenario, the presented method for SS generation offers an advantage with respect to the classical chaos-based

solution, provided that a preliminary study on the influence of the stop-band width and depth in the SS profile is performed numerically to evaluate their optimal value.

Finally, Figs. 8 represents the expected performance of BEP^v as a function of SIR, showing its mean value and its variance for SNR= 20 dB and stop-band width equal to $0.03N/T$, and where $\rho = 0.62$, $f_0 = 0.1N/T$ and $U = 12$ in plots (a), (b), while $\rho = 0.65$, $f_0 = 0.4N/T$ and $U = 20$ in plots (c), (d). Overall, memory-m sequences offer an uniform variance reduction and a general performance improvement in most operating conditions.

6. Conclusion

In this paper we presented a simple method to reduce the impact of a narrowband interference in UWB systems based on asynchronous DS-CDMA. The starting point is given by existing techniques reducing multi-access disturbances by appropriate chaos-based spreading codes. Then, the method is focused on shaping power spectral density of spreading sequences, made by symbols generated by LPFPs.

Power spectral shaping reduces the UWB information signal in the NBI frequency band, yielding a heavy reduction of the interference due to overlapping narrowband transmission. This however causes an increment in multi-access disturbance with respect to chaos-based spreading that minimizes MAI, thus implying a trade-off between rejection of narrowband interference and tolerance of multi-access interference.

Such a trade-off can be effectively address for different system configurations depending on the number of simultaneous users on the channel, the relative position of the UWB and narrowband spectra, and on the ratio between the power of the localized interferer and the power of UWB signal.

Numerical results reveal non-negligible improvements since, whenever SIR$\geq$ 5dB, $U \geq 20$ and $N = 128$, we found that memory-m sequences guarantee a lower average BEP^v, as well as an higher probability to reach any given quality link.

Note that in this paper we have assumed that the NBI frequency is fixed and know, as well as its power and the number of users in the system. As long as these parameters are unchanged, we have shown how to generate spreading sequences in order to maximize system performance; this solution however does not ensure anymore the optimum working point when one of the above parameter changes.

In order to ensure the performance optimization also in the case of a change in one (or more) of the above parameters, spreading sequences statistical features should be recomputed as soon as environmental conditions change. This is certainly not a problem for new users added to the system, that may immediately work with optimized sequences. However, old users (i.e. users that use spreading sequences optimized for a different environmental setting) may work with performance that may be lower with respect to the reference case, i.e. when sequences are generated with an autocorrelation profile $A_k \approx (-2 + \sqrt{3})^k$ without taking into account any NBI. To cope with this, a sequence renegotiation policy has to be implemented.

References

[1] M.B. Pursley, "Performance evaluation for phase-coded spread-spectrum multiple-access communication–Part1: System analysis," *IEEE Trans. Commun.*, vol. 25, pp. 795–799, 1970.

[2] M.K. Simon, J.K. Omura, R.A. Scholtz, and B.K. Levitt, *Spread Spectrum Communications Handbook*, McGraw-Hill, New York, 1994.

[3] A. Giorgetti, M. Chiani, and M.Z. Win, "The effect of narrowband interference on wideband wireless communication system," *IEEE Transactions on Communications*, vol. 53, pp. 2139–2149, 2005.

[4] G. Setti, G. Mazzini, R. Rovatti, and S. Callegari, "Statistical modeling of discrete-time chaotic processes: basic finite-dimensional tools and applications," *Proceedings of the IEEE*, vol. 90, pp. 662–690, 2002.

[5] R. Rovatti, G. Mazzini, G. Setti, and A. Giovanardi, "Statistical modeling of discrete-time chaotic processes: advanced finite-dimensional tools and applications," *Proceedings of the IEEE*, vol. 90, pp. 820–841, 2002.

[6] T. Kohda and H. Tsuneda, "Even- and odd-correlation functions of chaotic chebyshev bit sequences for CDMA," *IEEE ISSSTA '94*.

[7] T. Kohda and A. Tsuneda, "Explicit evaluations of correlation functions of chebyshev binary and bit sequences based on perron-frobenius operator," *IEICE Trans. Fund.*, vol. E77-A, pp. 1794–1800, 1994.

[8] G. Mazzini, G. Setti, and R. Rovatti, "Chaotic complex spreading sequences for asynchronous DS-CDMA - Part I: System modeling and results," *IEEE Trans. Circ. Sys. - I*, vol. 44, pp. 937–947, 1997.

[9] R. Rovatti, G. Setti, and G. Mazzini, "Chaotic complex spreading sequences for asynchronous DS-CDMA - Part II: Some theoretical performance bound," *IEEE Trans. Circ. Sys.-I*, vol. 45, pp. 496–506, 1998.

[10] G. Maazini, R. Rovatti, and G. Setti, "Chaos-based asynchronous DS-CDMA," Chap 3 in *Chaotic Electronics in Telecommunications*, CRC Press, Boca Raton, pp. 33–79, 2000.

[11] R. Rovatti, G. Mazzini, and G. Setti, "Interference bounds for DS-CDMA systems based on chaotic piecewise-affine Markov maps," *IEEE Trans. Circ. Sys. - I*, vol. 47, pp. 885–896, 2000.

[12] G. Mazzini, R. Rovatti, and G. Setti, "Interference minimization by autocorrelation shaping in asynchronous DS-CDMA systems: Chaos-based spreading is nearly optimal," *Electronics Letters*, vol. 35, pp. 1054–1055, 1999.

[13] G. Setti, R. Rovatti, and G. Mazzini, "Synchronization mechanism and optimization of spreading sequences in chaos-based DS-CDMA systems," *IEICE Trans. on Fundamentals*, vol. E82-A, pp. 1737–1746, 1999.

[14] T. Kohda and H. Fujisaki, "Pursley's aperiodic cross-correlation functions revisited," *IEEE Trans. Circ. Sys. - I*, vol. 50, pp. 800–805, 2003.

[15] Y. Jitsumatsu and T. Kohda, "Bit error rate of incompletely synchronised correlator in asynchronous DS/CDMA system using SS Markovian codes," *Electronics Letters*, vol. 38, pp. 415–416, 2002.

[16] H. Fujisaki and H. Sugimori, "Phase-shift-free M-phase spreading sequences of Markov chains," *IEEE Trans. Circ. Sys. - I*, vol. 55, pp. 876–882, 2008.

[17] G. Cimatti, R. Rovatti, and G. Setti, "Chaos-based spreading in DS-UWB sensor networks increases available bit rate," *IEEE Transaction on Circuits and Systems - Part I*, vol. 54, pp. 1327–1339, 2007.

[18] R. Rovatti, G. Mazzini, and G. Setti, "A tensor approach to higher-order expectations of quantized chaotic trajectories - Part I: General theory and specialization to piecewise affine Markov systems," *IEEE Transaction on Circuits and Systems - I*, vol. 47, pp. 1571–1583, 2000.

[19] G. Mazzini, R. Rovatti, and G. Setti, "A tensor approach to higher-order expectations of quantized chaotic trajectories - Part II: Application to chaos-based DS-CDMA in multipath environments," *IEEE Transaction on Circuits and Systems - Part I*, vol. 47, pp. 1584–1596, 2000.

[20] R. Rovatti, G. Mazzini and G. Setti, "Enhanced rake receivers for chaos-based DS-CDMA," *IEEE Transaction on Circuits and Systems - Part I*, vol. 48, pp. 818–829, 2001.

[21] G. Mazzini, R. Rovatti, and G. Setti, "Chaos-based asynchronous DS-CDMA systems and enhanced Rake receivers: measuring the improvements," *IEEE Transaction on Circuits and Systems - Part I*, vol. 48, pp. 1445–1453, 2001.

[22] G. Setti, R. Rovatti, and G. Mazzini, "Performance of chaos-based asynchronous DS-CDMA with different pulse shapes," *IEEE Communications Letters*, vol. 8, pp. 416–418, 2004.

[23] G. Mazzini, G. Setti, and R. Rovatti, "Chip pulse shaping in asynchronous chaos-based DS-CDMA," *IEEE Transaction on Circuits and Systems - Part I*, vol. 54, pp. 2299–2314, 2007.

[24] Y. Jitsumatsu and T. Kohda, "Gaussian chip shaping enhances the superiority of Markovian codes in DS/CDMA systems," *Proceedings of the IEEE International Symposium on Circuits and Systems (ISCAS2006)*, pp. 3117–3120, 2006.

[25] Y. Jitsumatsu, M. Ogata, and T. Kohda, "A comparison between prolate spheroidal and Gaussian FIR pulse shaping filters," *Proceedings of the International Conference on Signals and Electronic Systems (ICSES2008)*, pp. 343–346, 2008.

[26] R. Rovatti, G. Mazzini, and G. Setti, "On the ultimate limits of chaos-based asynchronous DS-CDMA - I: Basic definitions and results," *IEEE Transaction on Circuits and Systems - Part I*, vol. 51, pp. 1336–1347, 2004.

[27] R. Rovatti, G. Mazzini, and G. Setti, "On the ultimate limits of chaos-based asynchronous DS-CDMA - II: Analytical results and asymptotics," *IEEE Transaction on Circuits and Systems - Part I*, vol. 51, pp. 1348–1364, 2004.

[28] M. Mangia, R. Rovatti, and G. Setti, "Narrowband interference reduction in UWB systems based on spreading sequence spectrum shaping," *Procedings of the IEEE Internations Symphosium on Circuits and Systems (ISCAS2010)*, pp. 1799–1802, 2010.

[29] J.S. Lehnert and M.B. Pursley, "Error probabilities for binary direct-sequence spread-spectrum communication with random signature sequence," *IEEE Trans. Commun.*, vol. COMM-35, pp. 87–98, 1987.

[30] R. Rovatti, G. Mazzini, and G. Setti, "Memory-m antipodal processes: spectral analysis and synthesis," *IEEE Transaction on Circuits and Systems - Part I*, vol. 56, pp. 156–167, 2009.

[31] R. Rovatti, G. Mazzini, G. Setti, and S. Vitali, "Linear probability feedback processes," *Procedings of the IEEE Internations Symphosium on Circuits and Systems (ISCAS2008)*, pp. 458–551, 2008.